Optical Engineering

SPIEDigitalLibrary.org/oe

Adaptive scale smoothing for road redundancy region elimination

Zhijian Huang
Jinfang Zhang
Jiaze Wu
Fanjiang Xu

SPIE

Adaptive scale smoothing for road redundancy region elimination

Zhijian Huang
National University of Defense Technology
School of Electronic Science and Engineering
Kaifu District, Changsha 410073, China
and
Institute of Software
Chinese Academy of Sciences
IIST Key Laboratory
Zhongguancun, Beijing 100190, China
E-mail: zhijian07@iscas.ac.cn

Jinfang Zhang
Jiaze Wu
Fanjiang Xu
Institute of Software
Chinese Academy of Sciences
IIST Key Laboratory
Zhongguancun, Beijing 100190, China

Abstract. In the process of road extraction, the road region often mixes with some redundancies caused by the phenomenon of "different objects with the same spectrum," which exists widely in remote sensing images. To eliminate these redundancies and preserve neat and accurate road regions, a method based on skeleton analysis is proposed. At first, the shortest path of a specified road segment is constructed with mixed region skeletons. The road width at the skeleton point is then selected as the smoothing scale on this point, on which basis an accumulative and bidirectional smoothing is taken. With the smoothed path and its average width, a buffer algorithm reconstructs the road region. The results show that redundancies of the road can be eliminated correctly, and accurate road center lines and neat road regions can be obtained. [DOI: 10.1117/1.OE.51.6.066201]

Subject terms: road extraction; skeleton analysis; shape characteristic; spectrum characteristic; adaptive scale smoothing; remote sensing image.

Paper 120173 received Feb. 9, 2012; revised manuscript received Apr. 6, 2012; accepted for publication Apr. 11, 2012; published online Jun. 5, 2012.

1 Introduction

Object-based image analysis (OBIA) is an inevitable trend in remote sensing image analysis.[1] Meaningful objects, that is, regions with closed contours, are the foundation of OBIA. Accurate segmentation is a prerequisite for extracting a set of meaningful objects. However, it is difficult to realize, because the phenomenon of "different objects with the same spectrum" exists widely in remote sensing images. Meaningful objects often mix with some redundancies, as shown in Fig. 1, where the road is mixed with a house and some other regions. This experiment aims to separate an object from a mixed one and reshape it into a truly meaningful object, especially with regard to roads.

Some mathematic morphology algorithms[2,3] have been proposed to solve this problem. A series of open and closed operations with some structure elements can separate an object at a narrow position and smooth its contours. However, selecting an appropriate structure element is difficult. When the object is narrow, for instance roads, it will be cut falsely into many small parts, as, seen in Fig. 2(b). When the redundant region is large and coheres to a road region closely, for example the red rectangle in Fig. 2(a), these algorithms cannot also separate the road from a mixed object.

Since different parts of the mixed object have a similar spectrum and texture characteristics, redundant region elimination should make full use of shape information. Researchers[4] segmented the road group, which is the result of a supported vector machine (SVM) Classifier, into geometrically homogeneous objects with a multiresolution segmentation algorithm integrated in eCognition. Road objects are then selected with an simple thresholding on the shape index and density. The assumption is that a road object should have large values of shape index and small values of density. In fact, this assumption is not true for every situation. Many non-road objects also satisfy these conditions, while some road objects do not satisfy them. The reason is that shape index and density cannot represent a road object uniquely and robustly.

The skeleton is important for object representation and recognition in different areas, such as image retrieval,[5] shape classification,[6–8] and object detection.[9] A skeleton-based hypothesis is proposed in Ref. 10. The assumption is that the width of roads does not vary abruptly. A single thresholding is then taken, which uses only the average and the variance of skeleton branch widths to decide whether or not this branch should be reserved.

Different from the assumption in Ref. 10, we assume that the width of the road region is locally constant and that the road center line is smooth and the shortest path composed by its skeletons. State-of-art methods for skeleton extraction and pruning have been presented.[11–13] Here, pruned skeletons of a mixed object are extracted with the algorithm proposed in Ref. 13. Once the decision has been made to extract a road region by specifying its starting point and ending point from all the skeleton points, the shortest path is constructed with mixed region skeletons, followed by an adaptive scale selection. The scale of smoothing on different parts of this path is decided by the width of the road region at the current skeleton point. After an accumulative and bidirectional smoothing, a smooth road center line is obtained. With the smoothed road center line and its average width, a buffer algorithm reconstructs the road region. The experiment result is shown in Fig. 3, where the red line is the road center line, while the black region is the reconstructed road region. If there is an intersection and the width changes obviously, the operator can add a pair of start/stop points to avoid unnecessary error.

0091-3286/2012/$25.00

Fig. 1 Phenomenon of "different objects with the same spectrum." (a) Initial image. (b) Mixed object consisting of a road and a house.

Fig. 2 (a) A mixed object. (b) The result of mathematic morphology with a disk construct element.

Fig. 3 Result of the proposed method.

2 Methodology

In our model, a road region is a strip with locally constant width. So the skeleton of a road region is just the road center line, with constant width at every skeleton point. Unfortunately, the actual situation is more complex than our model. On one hand, noise in the object contour causes some small branches even though the skeletons are pruned. On the other hand, the road region mixes with some redundant regions (usually a house roof, park, or bare land) that have a similar spectrum and texture characteristics as the former. At the position where the road region is connected by a large redundancy, its width increases abruptly, forming a bend called a merging bend, as seen in Fig. 4(a).

To solve these problems, this paper constructs the shortest path [the white line in Fig. 4(b)] with skeletons of the mixed region by specifying its starting point and ending point. An accumulative and bidirectional smoothing with adaptive scale is then taken to obtain a smooth road center line. At last, with the smoothed road center line and its average width, a buffer algorithm reconstructs the road region.

2.1 *Adaptive Scale Selection*

The shortest path can be represented as an ordered collection of skeleton points: $\boldsymbol{P} = \{p_i | p_i = (x_i, y_i, w_i); i = 1, 2, \ldots, N\}$, where N is the number of the path's skeleton points and w_i is the radius of road region at p_i, which means the least distance from p_i to the object contour. The x coordinates can be represented as a sequence $x(i) = \{x_i | i = 1, 2, \ldots, N\}$, and y coordinate $y(i) = \{y_i | i = 1, 2, \ldots, N\}$, respectively. Usually, a Gaussian kernel $g(u, \sigma) = \exp\{-|u - u_0|/2\sigma^2\}$ is used to smooth the path, where variance σ, called a smooth scale, is a constant. The higher the σ is, the smoother the line will be. If the σ is too small, the Merging Bend cannot be smoothed, as seen from the green line in Fig. 5. In contrast, by smoothing the bend, other parts become distorted, as seen from the blue line in Fig. 5. No matter how this constant is chosen, the result is unsatisfactory.

Fig. 4 (a) Mixed object skeletons. (b) Shortest path.

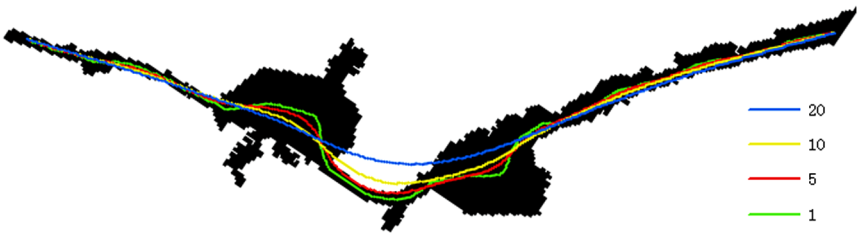

Fig. 5 Results with constant σ, taken as 1, 5, 10, and 20, respectively.

If the smooth scale σ is not a constant, the result may be more satisfactory. The wider the road region is at the current skeleton point is, the larger is the range of its neighborhood that will be used to decide its position. A good idea is that the neighborhood range of the current skeleton point is proportional to its radius. So the adaptive scale Gaussian kernel is

$$g(u, w_i) = \frac{1}{Z} \exp\left\{\frac{-|u-u_0|^2}{2(\sigma_0 w_i)^2}\right\}, \tag{1}$$

where $Z = \int \exp\{\frac{-|u-u_0|^2}{2(\sigma_0 w_i)^2}\} \mathrm{d}u$ is used as a normalization factor. In the experiments, σ_0 takes 1. The Gaussian kernel can be discretized as a sequence $g(j,i) = \{g(u_j, i) | j = -m, \ldots, m; i = 1, \ldots, N\}$, where m is decided by the maximum error that the user can accept. The position of the skeleton point $p_n = (x_n, y_n)$ after smoothed will be $\bar{p_n} = (\bar{x_n}, \bar{y_n})$, where

$$\bar{x_n} = \sum_{k=-m}^{m} x(n-k) g(k,n), \tag{2}$$

and

$$\bar{y_n} = \sum_{k=-m}^{m} y(n-k) g(k,n), \tag{3}$$

where $g(k,n)$ is the normalized Gaussian kernel, that is, $\sum_{k=-m}^{m} g(k,n) = 1$. After smoothed with the adaptive scale $\sigma_0 w_i$, a more satisfactory result than mentioned above will be obtained, as shown in Fig. 6(a). However, it is also imperfect; little distortion exists at the position of the merging bend. The real center line at this part should be adjusted toward the direction of the red arrow. An more obvious example is illustrated in Fig. 6(b).

2.2 *Accumulative and Bidirectional Smoothing*

To remedy the defect mentioned in Sec. 2.1, an accumulative and bidirectional smoothing algorithm is presented.

Different from the process above, the position of p_i is updated dynamically. Every time, once the new position of p_i is calculated with Eqs. (2) and (3), the sequence $x(i)$ and $y(i)$ is updated immediately. So the position of subsequent skeleton points in $\boldsymbol{P}$ is calculated with the updated sequence. This process is called accumulative smoothing. The result with the same road region as in Fig. 6(b) is shown in Fig. 7.

As seen from Fig. 7, distortion of the center line at the position of the left arrow in Fig. 6(b) is alleviated obviously. However, the distortion still exists on the right arrow. The reason is that accumulative smoothing is processed from left to right. If accumulative smoothing goes from head to tail, and then the reverse, the performance will improve remarkably. The result is described in Fig. 8.

2.3 *Road Region Reconstruction*

Once the road center line is fixed, the average width of the path can be calculated. By use of a buffer algorithm such as that integrated in ArcGis, the road region will be reconstructed quickly. The results of the examples mentioned above are shown in Fig. 9, where red lines denote road center lines, and white regions denote reconstructed road regions.

3 Results and Discussion

To analyze the performance of the proposed method, some large images have been taken into the experiment and compared with the method mentioned in Ref. 10. All the results are shown in Fig. 10.

(a) **(b)**

Fig. 6 Results of adaptive scale smoothing. (a) For the mixed region in Fig. 5. (b) For the mixed region in Fig. 4.

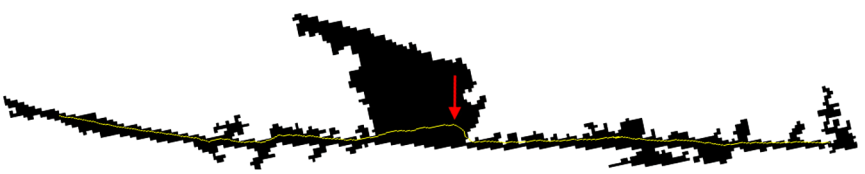

Fig. 7 Result with accumulative smoothing.

Fig. 8 Result of the proposed method.

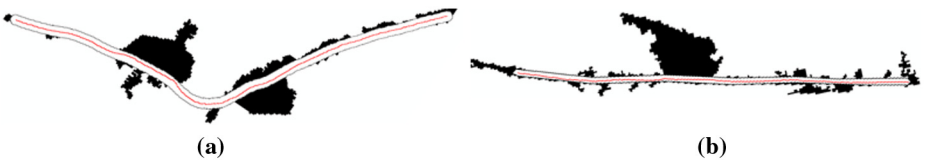

Fig. 9 Road regions reconstructed with buffer algorithm.

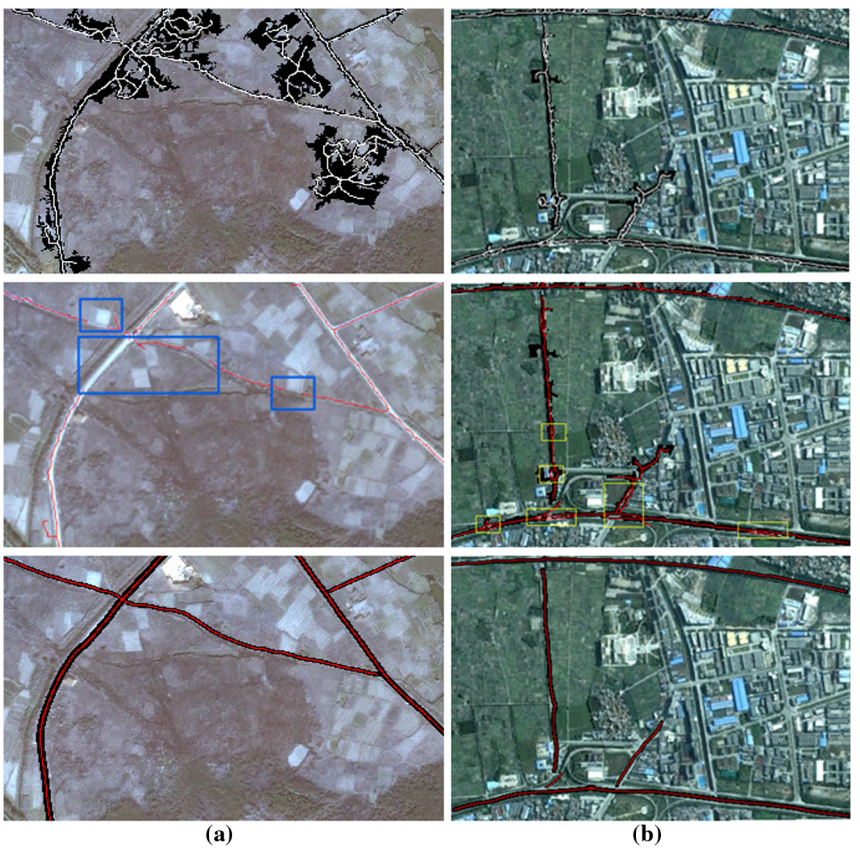

Fig. 10 (a) A suburb region in Shantou, 1173 × 651 pixels. (b) An urban region in Guangzhou, 2996 × 1980 pixels. (*top*) Road regions (black regions) and skeleton (white lines). (*middle*) Results from Ref. 10 (red lines are road center lines). (*bottom*) Results of the present experiment (red lines are road center lines, black regions are the reconstructed road regions).

The results from Ref. 10 are shown in the middle row of Fig. 10. Although most branches of redundancies have been removed, there are still some problems, such as an unsmoothed disconnection (yellow rectangle), false detection (blue rectangle), and spurs. The main cause of these problems is that only a single thresholding is taken, which uses width average and variance of skeleton branch to decide whether or not this branch should be reserved. Obviously, single thresholding can hardly to distinguish a road region with its redundancies.

Results of the present experiment exhibit good performance. First, redundant regions with a spectrum and texture characteristics similar to those of the road region are removed correctly, which alleviates the effect of "different objects with the same spectrum" phenomenon. Second, road center lines are smooth, at accurate position, and complete. Last, reconstructed road regions are close to the real ones and have smooth and neat contours. The good performance benefits from three aspects. Above all, a semi-automatic method is used to determine which road region to extract, by specifying its starting point and ending point from all the skeleton points, easing the problem of distinguishing the road region from the non-road region. Moreover, the adaptive smoothing which selects different scale according different road width can

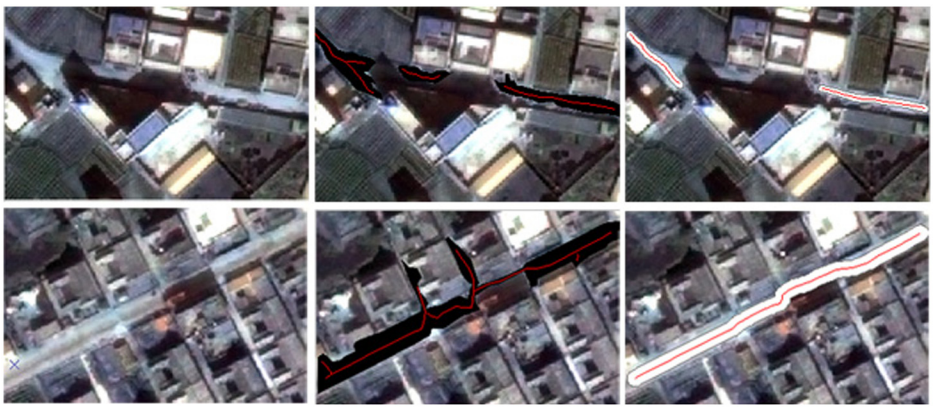

Fig. 11 Results of roads with complete occlusion (*top row*) and incomplete occlusion (*bottom row*). The first column contains initial images; the second shows the road region (black) and skeletons (red line); and the third shows the road center line (red) and the reconstructed region (white).

make road center line move toward its real position and make it smooth. Finally, a buffer algorithm with a smooth road center line and its average width can reconstruct the road region with a neat and accurate contour.

As to occlusion, there are two situations: incomplete occlusion and complete occlusion. With regard to the first situation, although the width changes obviously and is not locally constant, the occlusion can be jumped over, as shown in the bottom row of Fig. 11. However, when the road is occluded completely (as in the top row of Fig. 11), our algorithm cannot jump over it, which is one of the focuses of our future work.

However, there are also some defects, which are the focus of our future work. The first one is that the method is not completely automatic, but need to specify the start point and end point of a road region from its skeleton points. The second one is that our algorithm can not jump over the complete occlusions caused by trees, cars and buildings.

4 Conclusion and Future Work

Since road regions are often mixed with some redundancies (house, park, or bare land) because of the phenomenon of "different objects with the same spectrum," elimination of redundancies is necessary for future work. To obtain a neat and smoothed road region, a method based on skeleton analysis is proposed in this paper. At first, the shortest path of a specified road segment is constructed with mixed region skeletons. Then the width of the skeleton point is selected as the smoothing scale on the current point, on which basis an accumulative and bidirectional smoothing is taken. With the average width and the smoothed path, a buffer algorithm reconstructs the road region. The presented experimental results demonstrate that road redundancies can be eliminated correctly. Compared with a method proposed by others, the extracted road center lines are more complete and smoothed. The reconstructed road regions are also neat and accurate.

Our future work will concern extracting the road center line and reconstructing the road region without any interaction, jumping complete occlusions caused by trees and buildings, and making the results more complete.

References

1. E. S. Malinverni et al., "Hybrid object-based approach for land use/land cover mapping using high spatial resolution imagery," *Int. J. Geogr. Inform. Sci.* **25**(6), 1025–1043 (2011).
2. C. Zhu et al., "The recognition of road network from high-resolution satellite remotely sensed data using image morphological characteristics," *Int. J. Rem. Sens.* **26**(24), 5493–5508 (2005).
3. P. Soille and M. Pesaresi, "Advances in mathematical morphology applied to geoscience and remote sensing," *IEEE Trans. Geosci. Rem. Sens.* **40**(9), 2042–2055 (2002).
4. M. Song and D. Civco, "Road extraction using SVM and image segmentation," *Photogramm. Eng. Rem. Sens.* **70**(12), 1365–1371 (2004).
5. S. Krinidis and V. Chatzis, "A skeleton family generator via physics-based deformable models," *IEEE Trans. Image Process.* **18**(1), 1–11 (2009).
6. B. Xiang et al., "Integrating contour and skeleton for shape classification," in *IEEE 12th International Conf. on Computer Vision Workshops (ICCV Workshops)*, IEEE Computer Society, Kyoto, Japan, pp. 360–367 (2009).
7. E. Aykut and T. Sibel, "A similarity-based approach for shape classification using aslan skeletons," *Pattern Recogn. Lett.* **31**(13), 2024–2032 (2010).
8. L. Kart-Leong and H. K. Galoogahi, "Shape classification using local and global features," in *Fourth Pacific-Rim Symposium on Image and Video Technology (PSIVT)*, IEEE Computer Society, Singapore, Singapore, pp. 115–120 (2010).
9. X. Bai et al., "Active skeleton for non-rigid object detection," in *12th International Conf. on Computer Vision (ICCV 2009)*, IEEE Computer Society, Kyoto, Japan, pp. 575–582 (2009).
10. S. Das et al., "Use of salient features for the design of a multistage framework to extract roads from high-resolution multispectral satellite images," *IEEE Trans. Geosci. Rem. Sens.* **49**(10), 3906–3931 (2011).
11. B. Xiang et al., "Skeleton pruning by contour partitioning with discrete curve evolution," *IEEE Trans. Pattern Anal. Mach. Intell.* **29**(3), 449–462 (2007).
12. A. D. Ward and G. Hamarneh, "The groupwise medial axis transform for fuzzy skeletonization and pruning," *IEEE Trans. Pattern Anal. Mach. Intell.* **32**(6), 1084–1096 (2010).
13. W. Shen et al., "Skeleton growing and pruning with bending potential ratio," *Pattern Recogn.* **44**(2), 196–209 (2011).

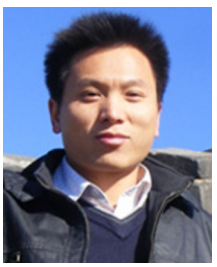

Zhijian Huang received the BSc from the School of Telecommunication Engineering, Air Force Engineering University in 2006 and a MSc from the School of Electronic Science and Engineering, National University of Defense Technology (NUDT) in 2009. Currently, he is a doctoral candidate at NUDT.

Jinfang Zhang received BSc and MSc degrees from China University of Geosciences, in 1992 and 2002, respectively. Currently, he is an associate professor at the Institute of Software, Chinese Academy of Sciences.

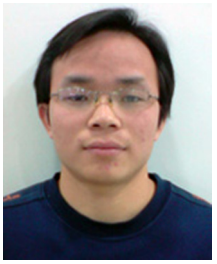

Jiaze Wu received a PhD in 2011 from the Institute of Software, Chinese Academy of Sciences. Now, he is an assistant researcher in the IIST Key Laboratory of the Institute of Software, Chinese Academy of Sciences. His research interests include image processing and analysis, real-time rendering, realistic rendering, virtual reality, and optical simulation.

Fanjiang Xu is a professor at the Institute of Software, Chinese Academy of Sciences.